The International Supercritical CO_2 Energy Technologies Symposium
March 2 - 5, 2026, Pittsburgh, PA
Paper #053

Comparison of sCO_2 Compressor Performance Test Results Using Temperature-, Density-, Or Torque-based Measurements

Craig Nolen
Senior Research Engineer
Southwest Research Institute
San Antonio, Texas

Katherine Bentley
Research Engineer
Southwest Research Institute
San Antonio, Texas

George Khawly
Research Engineer
Southwest Research Institute
San Antonio, Texas

Wade Mao
Engineer II
GTI Energy
Des Plaines, Illinois

Craig Nolen is a Senior Research Engineer in the Machinery Department at Southwest Research Institute, where he has been heavily involved in the U.S. Department of Energy's STEP 10 MWe sCO_2 Pilot-Scale Demonstration Power Plant project for over 7 years. His experience in this role has included facility design and construction, electrical equipment installation, instrumentation and data acquisition system development, system commissioning, and more. Prior to working on the STEP project, he was involved in thermal-mechanical FEA, thermodynamic cycle modeling, and development of novel test set ups for various clients. He has both B.S. and M.S. degrees in Mechanical Engineering from Texas A&M University.

George Khawly is a Research Engineer in the Power Cycle Machinery Section at Southwest Research Institute and licensed Professional Engineer in the state of Texas. He has experience in modeling thermal cycles utilizing and developing the Numerical Propulsion System Simulation framework (NPSS) for design, off-design, and transient operations. He has been assisting the Supercritical Transformational Electric Power Pilot Plant, a 10 MWe super-critical carbon dioxide pilot plant, during which he has been performing subsystem analysis, design, and integration and is the valve lead engineer within this project.

Kat Bentley is a Research Engineer in the Power Cycle Machinery Section at Southwest Research Institute, where she has been involved in the U.S. Department of Energy's STEP 10 MWe sCO_2 Pilot-Scale Demonstration Power Plant project for just under a year. Her contributions include instrumentation and data acquisition system development, plant operations control coding, and auxiliary piping and insulation engineering support. Prior to her introduction to STEP, she was lead test engineer for a privately funded post process carbon capture project where she was integral in materials, test article, test cell, and test procedure design and data acquisition and processing. She has a B.S. in Mechanical Engineering from the University of Texas at San Antonio, and a M.S. in Engineering Systems Management from St. Mary's University.

Wade Mao is an Engineer II in the Process Engineering group at GTI Energy. Over the past three years, he has supported the U.S. Department of Energy's STEP 10 MWe supercritical CO_2 pilot project focusing on steady state modeling of the simple cycle and recompression Brayton cycle (RCBC) configurations using Flownex. His work has centered on model improvement, integration of component test data, and comparison of predicted and measured plant performance. Beyond the STEP program, his experience includes electrolyzer system design and operation, process modeling of advanced power cycles, and pilot plant operation. He holds a B.S. degree from the University of Iowa and an M.S. degree from Columbia University, both in Chemical Engineering.

ABSTRACT

Determination of compressor performance in sCO_2 power cycles can pose a challenge if the inlet conditions are close to the critical point of sCO_2. In this region, density is very sensitive to temperature, so the inherent uncertainty with many temperature measurement methods can lead to relatively high uncertainty in performance parameters. For the main compressor of the STEP Demo 10 MWe sCO_2 plant, multiple different measurements were made to help determine compressor performance: inlet temperature, inlet density, and drive torque. This paper compares the results using these different measurements to help determine whether density-based or other methods can provide more reliable measurements than temperature for sCO_2 compressor performance.

INTRODUCTION

The engineering study of supercritical CO_2 as a power cycle working fluid continues to gain attention due to its promises of increased thermodynamic efficiency and reduced machinery size and its relatively benign and abundant nature. Several small- and pilot-scale demonstrations have increased the technology readiness level of sCO_2 power systems, and several companies have begun to attempt to commercialize the technology. [3, 4, 5]

Designing machinery for operation with sCO_2, in addition to the numerous benefits, also poses many technological challenges. For instance, the critical point for CO_2 is approximately 73.8 bar. Given that sCO2 power cycles typically operate fully above or near the critical point, even the cycle's low-pressure side hardware must be rated to a relatively high pressure. Depending on the compressor pressure ratio, the high side pressure can be 250 bar or more. These high pressures can pose challenges for pressure vessels and piping and also have serious ramifications for hardware such as vent valves, where the large pressure drops can result in significant Joule-Thomson cooling. The high pressure combined with a high turbine inlet temperature also poses a materials challenge, as only select materials can economically provide pressure containment at the conditions proposed for these cycles.

For many sCO_2 power cycles, cycle and compressor efficiency is best when compressor inlet conditions are very near the critical point. However, fluid properties such as density and speed of sound begin to change rapidly as conditions approach the critical point. Small changes in temperature or pressure can result in very large swings in density. For example, at 74 bar, a 2ºC shift in temperature from 32ºC to 30ºC results in a fluid density more than double its original value. If conditions decrease too low, the CO_2 can drop into its vapor dome and form liquid droplets. These droplets can cause significant damage to the high-speed compressor impeller, such as blade erosion and serious vibration issues. In order to avoid liquid formation, temperature and pressure must be carefully controlled and monitored at the compressor inlet.

Besides the risk of physical damage to the system, operating near the critical point also poses a challenge for temperature measurements. When measuring fluid temperature in a flowing pipe, the measured temperature is typically somewhere between the total and static temperatures due to flow disturbances created around the probe or thermowell. The recovery factor of a probe mathematically relates the measured temperature to the total and static temperatures and enables their calculation. ASME PTC-10 defines recovery factor as a coefficient relating measured and static enthalpies and the kinetic energy of the fluid flow, which has the same effect. Typical methods for predicting the recovery factor of thermowells do not account for the real gas behavior of CO_2 near its critical point, and thus there is increased uncertainty in the temperature measurements. Without test data to validate recovery factors for a specific thermowell design and operating conditions, assumptions must be made in the calculation of static and total temperature.

The STEP 10 MWe Pilot Scale sCO_2 Power Plant is a U.S. Department of Energy (DOE) funded project led by GTI Energy in partnership with Southwest Research Institute (SwRI) and GE Global Research. The project's goal is to design, build, and operate a pilot scale (10 MWe net output) sCO_2 power plant on SwRI's campus in San Antonio, Texas. [1] The plant successfully completed simple recuperated Brayton cycle testing in October 2024, generating approximately 4 MW of net electric power. This is the highest power sCO_2 cycle demonstration in the world. [2] After this success, the project then focused on reconfiguring for a recompression closed Brayton cycle configuration. Figure 1 shows a rendering of the STEP facility.

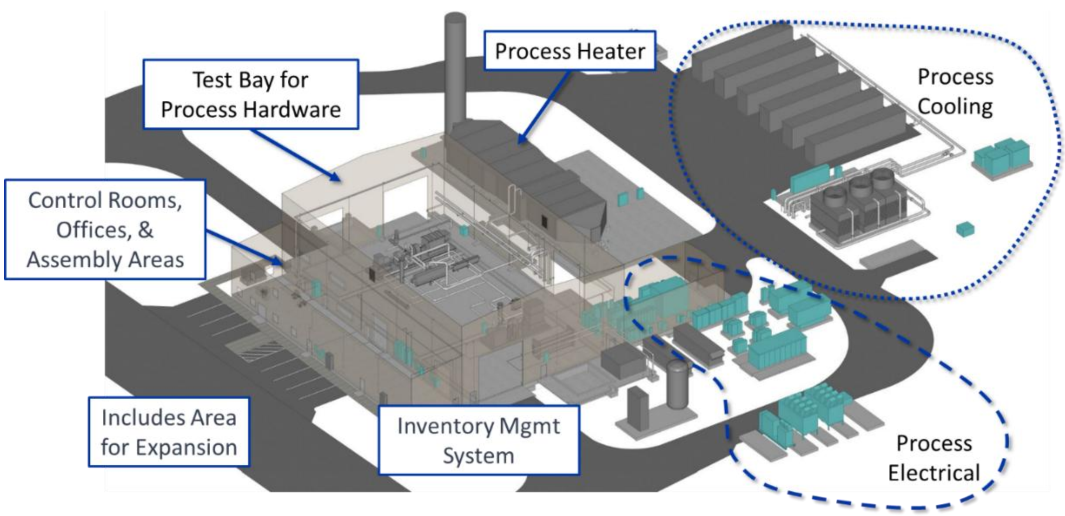

Figure 1. Preliminary 3D Rendering of STEP Facility

The plant includes two compressors, two recuperators, an externally fired natural-gas heater, a turbine, and water coolers as part of the cycle. Figure 2 shows a PFD of the cycle. In the simple recuperated configuration tested in October 2024, the bypass compressor and low-temperature recuperator were not installed. Jumper piping was installed to replace the LTR and maintain high- and low-pressure side flow continuity, while the lines to the bypass compressor were blinded off. The bypass compressor is coupled to the turbine, while the main compressor operates independently, utilizing a motor to drive it.

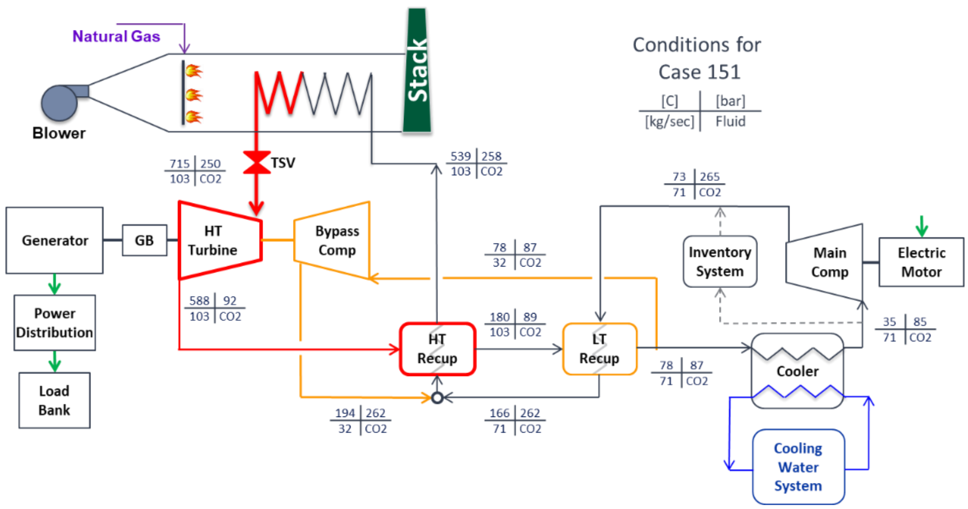

Figure 2. Recompression Closed Brayton Cycle Diagram

The STEP main compressor was designed and manufactured by Baker Hughes Nuovo Pignone and is a single-stage centrifugal machine with dry gas seals and oil-lubricated bearings. It is rated for approximately 3 MW of power but is driven by a 6 MW motor from a VFD. It has variable inlet guide vanes and vertically oriented suction and discharge piping. The main compressor is coupled to the motor utilizing a speed-increasing gearbox capable of achieving 27,000 rpm from the 1,800 rpm motor. Figure 3 shows the main compressor as installed on its skid in the high bay.

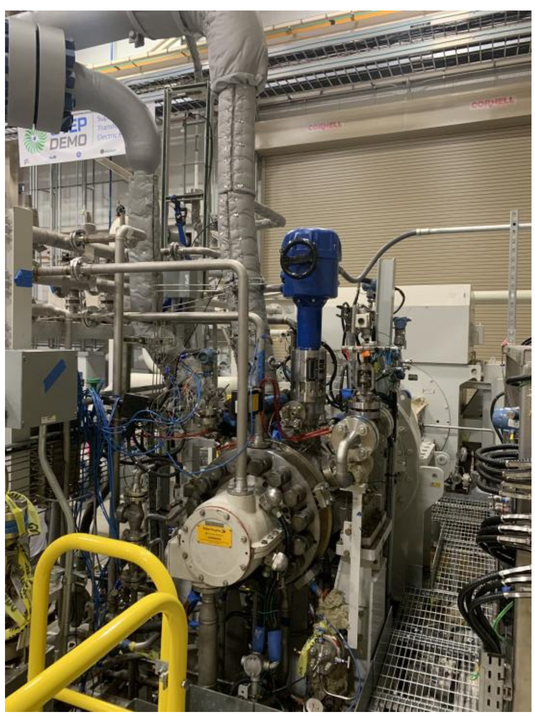

Figure 3. Main compressor with suction and discharge piping, gearbox, and motor

The main compressor experienced a wide range of operating conditions during the October 2024 testing. Because of the effects of temperature on fluid properties near the critical point, there were concerns that the temperature measurement uncertainty inherent to thermocouples might lead to increased uncertainty in the compressor performance calculations. Several different methods were used to attempt to measure the true inlet conditions and thus accurately determine compressor performance. Temperature and density were measured at the compressor inlet. Torque was measured in the low-speed coupling between the compressor's gearbox and motor. This paper explores the use of these different measurements in determining compressor performance for the STEP plant and attempts to show whether measurements other than temperature can reduce uncertainty in sCO_2 compressor performance testing.

METHODS

The STEP Demo plant has over 600 pressure and temperature instruments installed and monitored by its controls and data acquisition systems, and more than 1200 I/O points when control and feedback signals are included. Process control loops are required to maintain pressure and temperature set points at various points within the system. Vibration monitoring of spinning components is needed in order to quickly halt the process if vibrations exceed some nominal level, which could risk damaging equipment. As a research facility, some measurements installed, such as process pressure, temperature, and flow, are in a relatively larger quantity than is typical for a commercial application.

At this scale, an order of magnitude above typical lab-scale demonstrations, the number of interconnected sub-systems, control parameters, and instrumentation included in the plant design required a unique architecture for the controls and data acquisition system. The desire for the robustness and scalability of a commercial control system led to the purchase of a GE Mark VIe Distributed Control System (DCS) that serves to control and protect the plant during operation. The desire for measurement accuracy and flexibility in the computation and display of performance parameters led to the purchase of a separate NI LabVIEW-based Data Acquisition (DAQ) system that serves to provide high-accuracy, real time performance metrics as well as robust and reliable data storage for post-processing.

The main compressor was instrumented according to the guidelines of the ASME PTC-10 Compressor Performance Test Code as closely as possible, with inlet and exit temperature and pressure measurements installed in the suction and discharge piping. Recommended upstream and downstream installation distances were respected as much as possible (given pipe routing limitations) for all measurements. Four temperature probes and four static pressure taps were present in both suction and discharge piping. Each probe or measurement location of the same kind was spaced 90 degrees apart circumferentially from its neighbors. Orifice plate differential pressure flow meters were installed in the compressor discharge and recycle piping far downstream of the compressor. The discharge flow measurement location was upstream of the recycle measurement in order to capture the full flow rate coming out of the compressor. In Figure 4, the static pressure sensing lines on the suction piping can be seen routed away from the machine. The temperature measurement probes are also visible. Both suction and discharge piping were insulated with removable soft jackets.

Figure 4. Suction and discharge piping instrumentation

Temperature measurements were made using Omega T-type thermocouples with a rated uncertainty of +/-1ºC. End-to-end loop calibrations were performed on the thermocouples to reduce their uncertainty, shown for individual instrument locations in Table 1 below. Pressure measurements were made using Keller Valueline pressure transducers with a rated uncertainty of 0.1% (full span, 0-400 bar). End-to-end uncertainty for pressure measurements is shown in Table 1 below. Differential pressure measurements in the flow meter were made using Emerson Rosemount 3051S series sensors with a rated uncertainty of 0.035% (span). A torque meter was used to measure the torque in the compressor's low-speed shaft (between gearbox and motor) with a rated uncertainty of 0.02%. Compressor speed was measured using a keyphasor with a rated uncertainty of 0.03%. Compressor inlet density was measured using a Micromotion CDM100P Compact Density Meter with a rated uncertainty of 0.1 kg/m^3.

Table 1. Instrument Uncertainty Table

Measurement	Average End-to-End Uncertainty
Compressor Inlet Temperature	0.45%
Compressor Inlet Pressure	0.28%
Compressor Outlet Temperature	0.19%
Compressor Outlet Pressure	0.14%
Compressor Mass Flow Rate	0.64% (ASME MFC-3M estimate)
Compressor Low Speed Shaft Torque	0.02% (manufacturer's rating)
Compressor Speed Keyphasor	0.03% (manufacturer's rating for nominal compressor speed)
Compressor Inlet Density	0.1 kg/m3 (manufacturer's rating)

Estimates for the uncertainty of variables such as power and efficiency utilize the Kline-McClintock method. For REFPROP thermodynamic property values, calculations assume an uncertainty of 0.5%. In addition, in order to account for sensitivity to uncertainty of the state variables used for property reference, a Monte Carlo simulation was implemented for each REFPROP property. In this simulation, the uncertainties for the lookup values were used as the range of variation, and the 95% uncertainty was calculated for each property and added to the base 0.5% uncertainty. Mass flow uncertainty was calculated according to ASME MFC-3M for orifice plate differential pressure flow meters.

The compressor itself operates up to 27,000 rpm and is driven by an 1800 rpm electric motor through a speed-increasing planetary gearbox. A torque meter was installed on the low-speed coupling between the compressor's motor and gearbox. Knowledge of both speed and torque allows for a calculation of power transmitted through the shaft at the torque meter location. Because it is on the other side of the gearbox from the compressor, the power estimated with the torque meter does not include the power lost to transmission inefficiencies or windage in the gearbox or compressor bearings, seals, etc.

Figure 5 shows a section of the Piping and Instrumentation Diagram (P&ID) surrounding the main compressor, highlighting a selection of the instrumentation used to monitor its health and performance. Additional instrumentation is installed in the compressor itself and monitored by the compressor's dedicated control system.

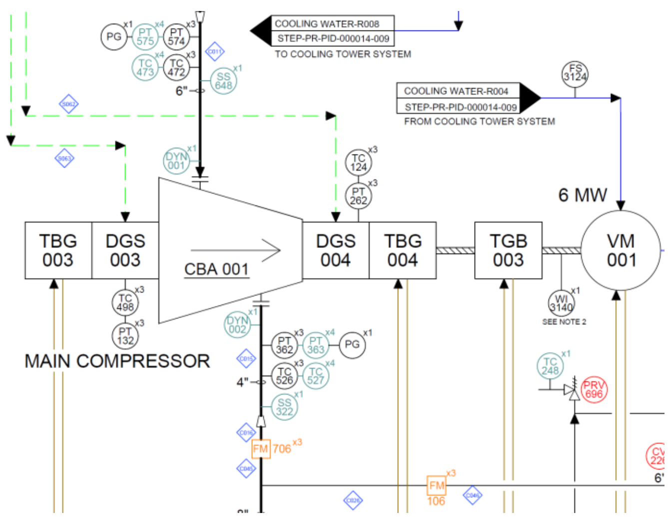

Figure 5. P&ID section around main compressor

During the test campaign in September and October 2024, a wide array of 29 steady-state performance test conditions was reached.

RESULTS AND DISCUSSION

For the temperature-based performance calculations, enthalpy values were calculated using REFPROP, while the state points provided were total temperature and pressure for each measurement location. Compressor power $\dot{W}$ is calculated using the difference in enthalpy between inlet and exit conditions (h_1 and h_2 respectively) as shown in equation 1. The isentropic efficiency η_s is calculated using equation 2 where h_{2s} represents the exit enthalpy, which is calculated assuming isentropic compression from the conditions of h_1. The value h_{2a} represents the actual measured enthalpy from pressure and temperature measurements and is the same as h_2.

$$\dot{W} = \dot{m}(h_2 - h_1) \tag{1}$$

$$\eta_s = \frac{h_{2s} - h_1}{h_{2a} - h_1} \tag{2}$$

For the density-based performance calculations, equation 1 is used for compressor power except inlet enthalpy value h_1 is calculated using the measured density and pressure rather than temperature and pressure. Exit enthalpy h_2 (and h_{2a} in equation 2) is calculated using temperature and pressure as before. In the efficiency calculation, the value of isentropic compression enthalpy h_{2s} is calculated starting from density-based h_1.

A sensitivity analysis was conducted to evaluate how small variations in main compressor inlet temperature and pressure influence compressor performance near the simple cycle operating range. Figure 6 through Figure 9 compare the predicted compressor power and isentropic efficiency across several inlet temperatures (about 35–37°C) and inlet pressures (about 84–90 bar) conditions. Both power and efficiency in the figures are normalized. The pressure and temperature on the x-axes are reported relative to a common reference condition. The compressor model used was based on operating maps derived from test data. The results highlight the high sensitivity of the main compressor when operating close to the critical point of CO_2. Even small changes of ±1°C or ±2 bar can cause noticeable shifts in both power and efficiency. At higher inlet temperatures or lower pressures, the fluid density decreases, which leads to higher volumetric flow and increased compressor power consumption. Lower temperatures or higher pressures represent higher density and reduce power requirements while increasing efficiency.

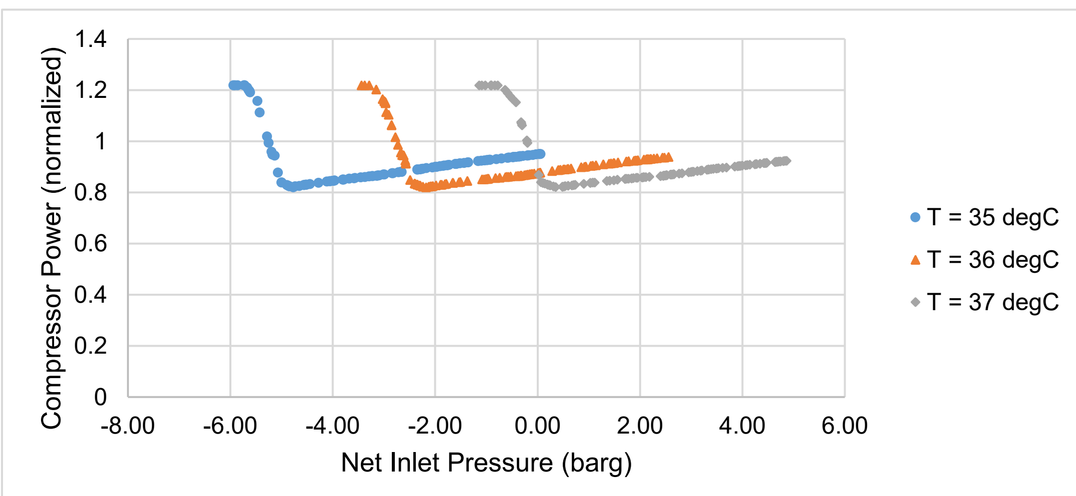

Figure 6. Normalized compressor model power (normalized) vs. net inlet pressure for different constant inlet temperatures

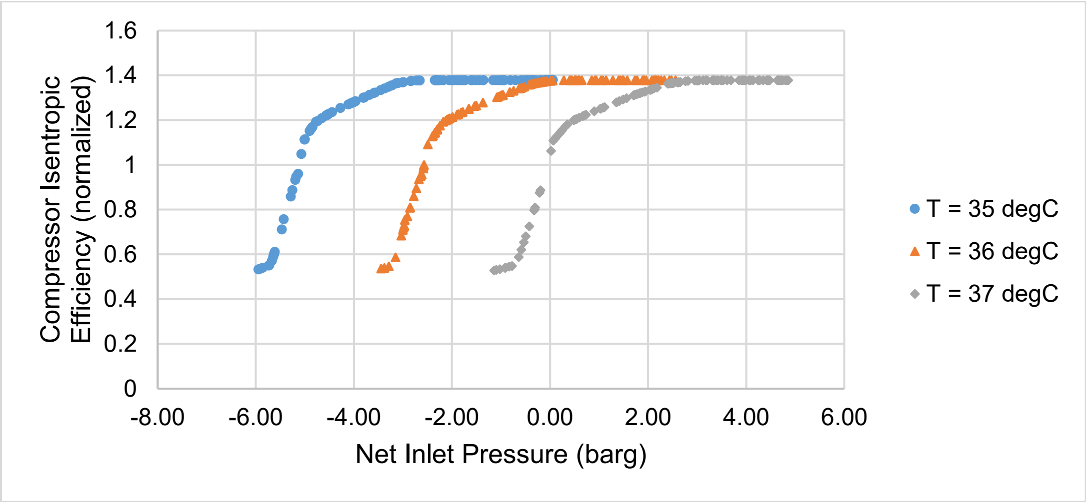

Figure 7. Compressor model efficiency (normalized) vs. net inlet pressure for different constant inlet temperatures

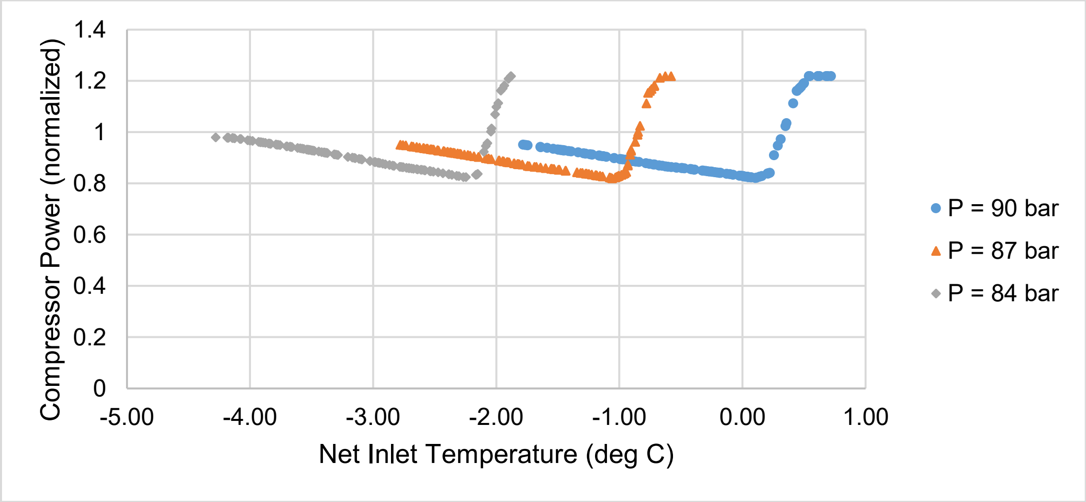

Figure 8. Compressor model power (normalized) vs. net inlet temperature for different constant inlet pressures

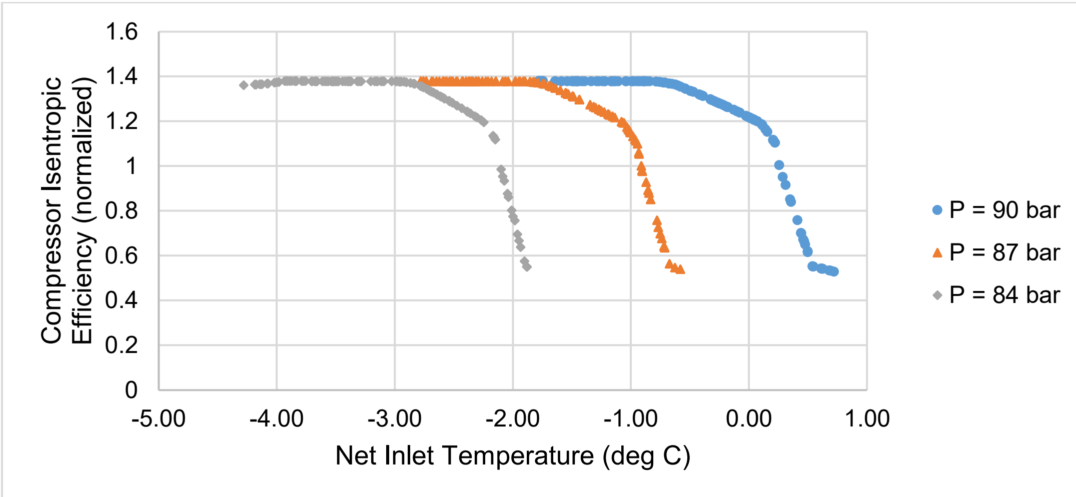

Figure 9. Compressor model efficiency (normalized) vs. net inlet temperature for different constant inlet pressures

Figure 10 shows the results of calculating compressor power using both temperature-based and density-based test measurements. The density-based power was, on average, 7.3% lower than the temperature-based power. The average uncertainty associated with the temperature-based method was 11.1%, while the average uncertainty associated with the density-based method was 7.0%.

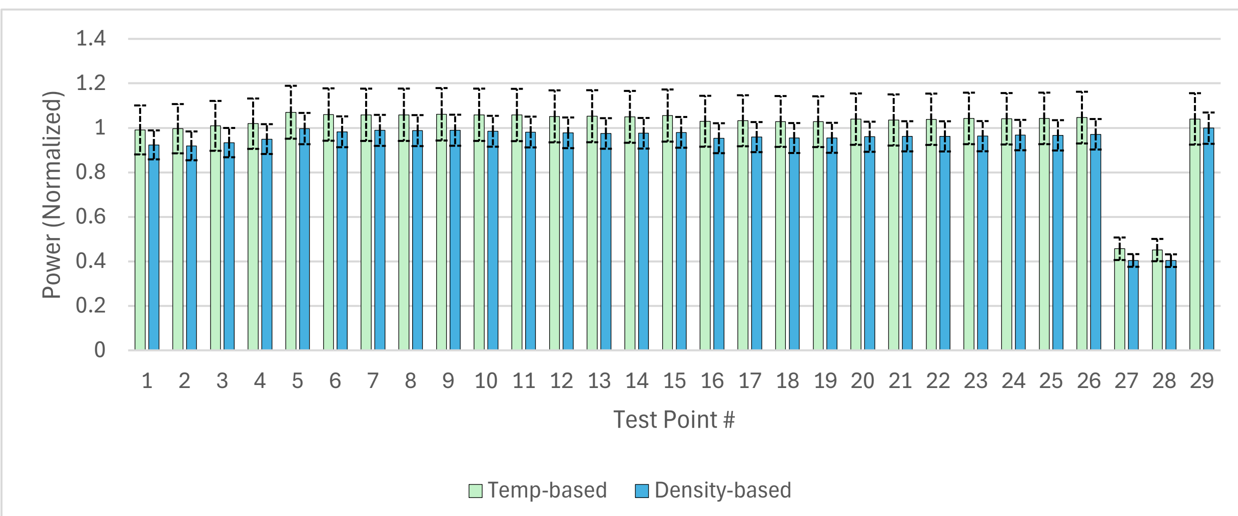

Figure 10. Compressor power (normalized) calculated using temperature-pressure vs using density-pressure

Figure 11 shows the results of calculating compressor efficiency using both temperature-based and density-based measurements. The density-based efficiency was, on average, 5% higher than the temperature-based efficiency. The uncertainty of the temperature-based efficiency was 10.7%, while that of the density-based efficiency was 6.7%.

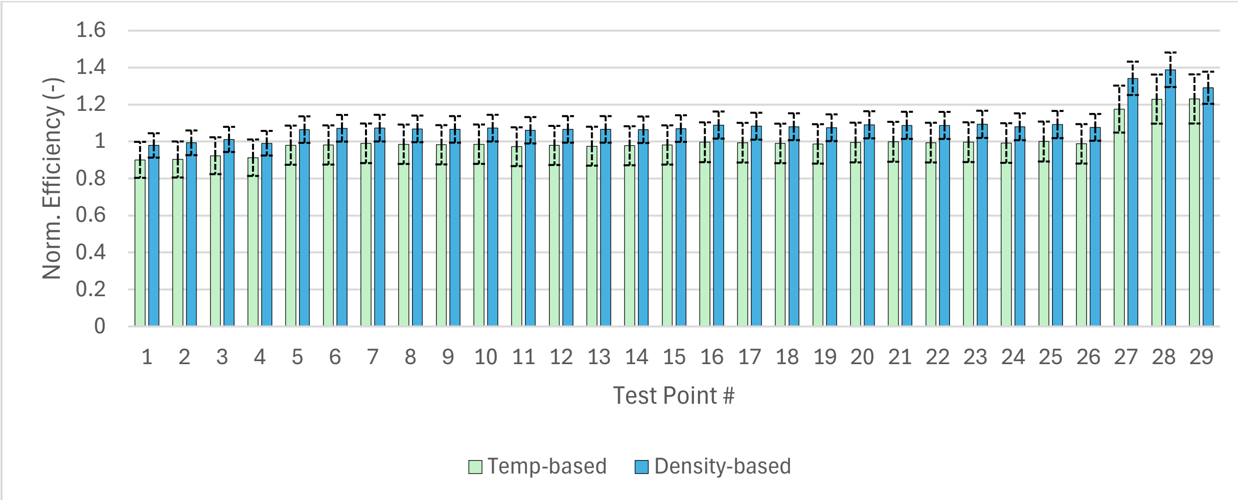

Figure 11. Compressor efficiency (normalized) calculated using temperature-pressure vs using density-pressure

The density-based method resulting in a lower power but higher efficiency can be explained by the relative change in inlet and exit enthalpy from the two methods. As seen in Figure 12, density-based inlet enthalpy is on average 0.8% higher than temperature-based. Since outlet enthalpy is the same for both methods, the higher inlet enthalpy of the density-based method results in a change in enthalpy that is 7.3% smaller in magnitude, explaining the difference in power.

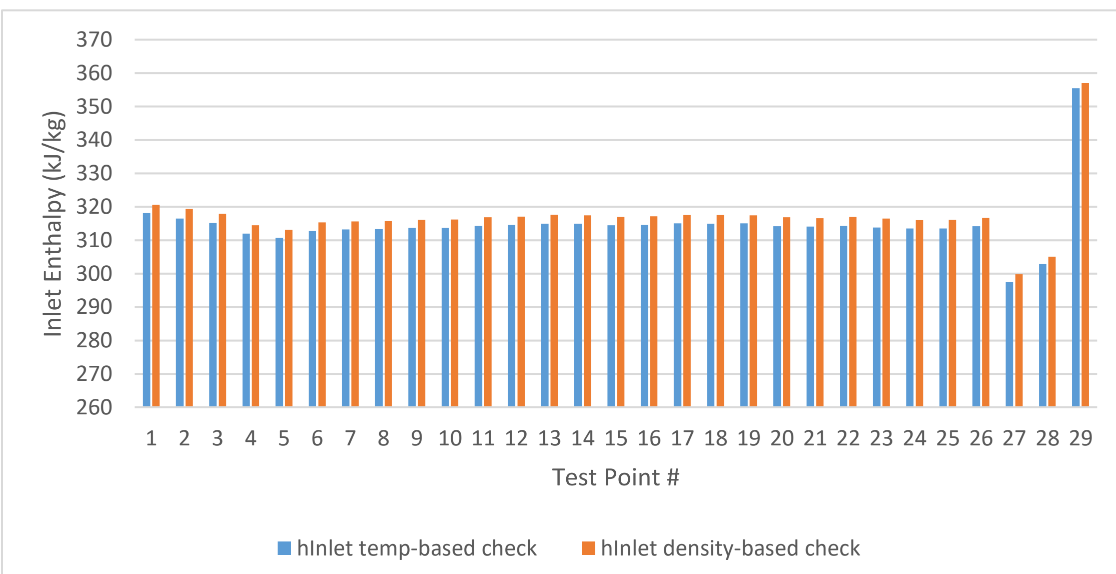

Figure 12. Compressor inlet enthalpy calculated using temperature-pressure vs using density - pressure

Figure 13 shows that the isentropic exit enthalpy was on average 0.8% higher for the density-based method, resulting in a change in isentropic enthalpy that was only 1.2% higher on average than the temperature-based method. A balance of this and the 7.3% smaller actual enthalpy change results in the observed 5% rise in efficiency.

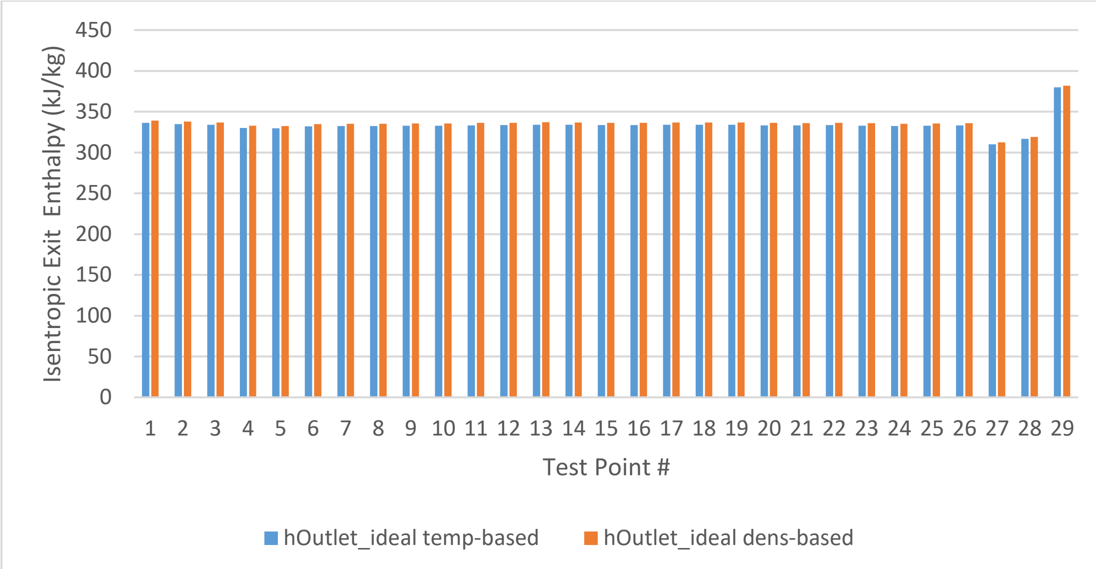

Figure 13. Compressor exit isentropic enthalpy calculated using temperature-pressure vs using density-pressure

The consistency of these differences across test points suggests a consistent bias in one method versus the other. The recovery factor for the thermowells used for temperature measurement are estimated to have a value of 0.7 which is used as part of the calculation of total temperature. Figure 14 shows the difference between total temperature calculated using density and pressure measurements and measured total temperature for all test points. The average difference is -0.3ºC. If the density-based data is true, and the temperature measurements adjusted accordingly, the actual recovery factor value is expected to be lower than 0.7 for the conditions tested.

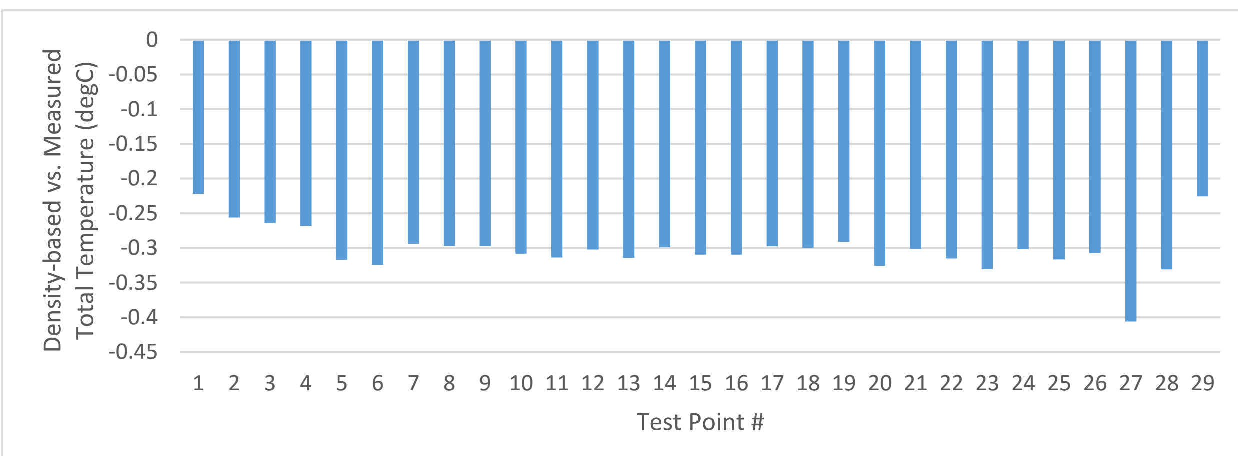

Figure 14. Difference between density-based and measured total temperature

Power transmitted through a shaft can be calculated as the product of torque and rotational speed according to Equation 3. With both torque and speed measurements available for the main compressor train low-speed shaft, it is possible to estimate power transmitted. However, because there are mechanical losses in the gearbox's and compressor's bearings, seals, shafts, etc., this estimate is expected to be biased higher than the actual value since it does not account for these losses.

$$\dot{W} = \tau\omega \quad (3)$$

Assuming 95% efficiency for both the gearbox and high-speed coupling, the actual power delivered to the compressor would be approximately 90% of what is measured at the low-speed coupling. This puts the torque-based power estimate somewhere between the temperature- and density-based estimates. Given the expectation of additional losses from the compressor bearings, seals, and shaft windage (not estimated), this estimate seems to align more closely with the density-based measurements. Placing uncertainty bars on the torque-based data shows an optimistic range for uncertainty, as it only accounts for the underlying measurement uncertainties and does not quantify the uncertainty of the assumed losses. Actual uncertainty about the presented data is expected to be higher.

It is also possible to use the torque-based power measurement to help estimate compressor efficiency without using inlet temperature by utilizing the steps below:

1. Calculate exit enthalpy: $h_{2a}(T_2, P_2)$
2. Use torque power to calculate inlet enthalpy:

$$h_1 = h_{2a} - \frac{\dot{W}_{torque}}{\dot{m}} \quad (4)$$

3. Calculate inlet entropy: $s_1(h_1, P_1)$
4. Calculate isentropic exit enthalpy: $h_{2s}(s_1, P_2)$
5. Calculate isentropic efficiency using equation 2: $\eta_s = \frac{h_{2s}-h_1}{h_{2a}-h_1}$

The torque-based power results are shown in Figure 15. Error bars are not shown because the instrument uncertainty for the torque and speed measurements were so small, the error bars were not visible compared to those for temperature and density-based measurements. However, this method clearly depends on the accuracy of the assumptions around the torque-based power number. If torque was measured directly on the compressor drive shaft, and data on compressor windage was available, it would be possible to reduce the uncertainty of the torque-based power estimate. Note that test points 28 and 29 did not have torque data.

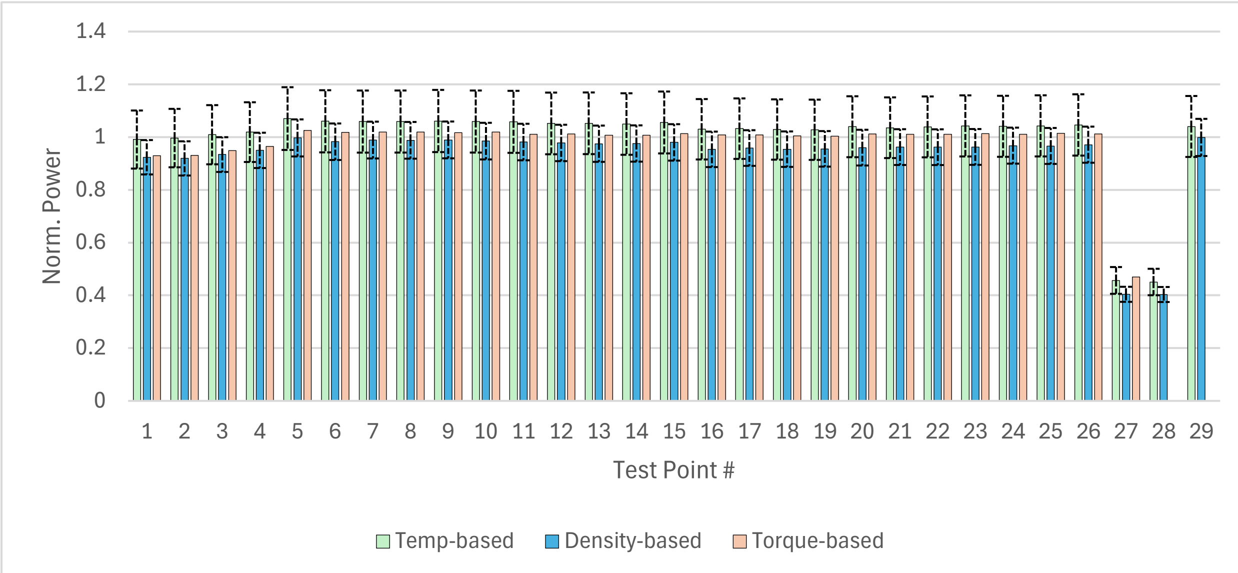

Figure 15. Compressor power with torque-based data

Torque-based efficiency results are shown in Figure 16. Similar to the power results, they are somewhere between the temperature- and density-based methods. These numbers are subject to the uncertainty concerns as for the torque-based power, as the same set of assumptions were used for estimating losses.

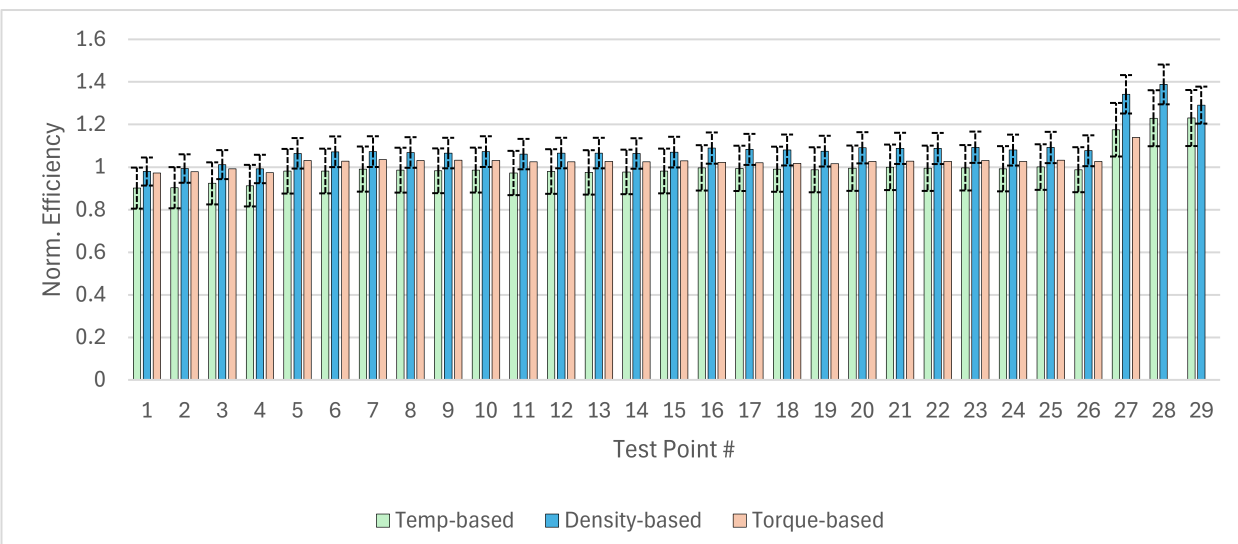

Figure 16. Compressor efficiency with torque-based data

Overall, the density-based performance calculations showed improved uncertainty relative to the other methods in this study. Lower uncertainty, however, does not necessarily imply increased accuracy. Density measurement, like temperature measurement, must be implemented correctly according to the manufacturer's recommendations and industry best practices. The density meter used in this study required a side stream pulled away from the main flow for measurement, so this line had to be designed in such a way that temperature did not change significantly from the bulk flow at time of measurement. The fact that the side stream had to be pulled far upstream of the inlet temperature and pressure measurements (to avoid inlet flow disturbances) also means that the fluid condition could have changed significantly between inlet density and pressure measurements. A density measurement that does not require a side stream or does not disturb the flow, such as a gamma ray densitometer, would reduce any effect of property changes between density and pressure measurements and still allow sufficient upstream distance to avoid flow disturbances at the compressor inlet.

Torque-based calculations could show greatly reduced uncertainty if windage losses are measured and properly accounted for, as the torque and speed measurements themselves typically have low uncertainty. However, difficulty in measuring bearing heating, windage in seals, flow leakage, casing heat loss to atmosphere, etc. can create a great degree of unquantified uncertainty. Installing the torque-meter as close as possible to the compressor (i.e., not opposite a gearbox) and measuring lube oil temperatures and flow rate could help reduce the overall uncertainty of this method.

CONCLUSION

Simulation of the compressor performance across a range of inlet conditions showed drastic changes in power efficiency with small changes in temperature, emphasizing the need to reduce uncertainty for inlet condition monitoring. The temperature and density-based calculation methods employed showed power results within 7.3% of each other. The density-based power method saw a 37% reduction in uncertainty relative to the temperature-based method. Temperature- and density-based efficiency results were within 5% of each other, and the density-based efficiency method also saw a similar 37% reduction in uncertainty. These results suggest that using density and pressure measurements for compressor inlet conditions can be superior to temperature and pressure measurements for sCO_2 compressors. Torque-based methods have relatively low instrument uncertainty, but many assumptions and supporting data are needed to reach performance estimates. This can lead to uncertainty that is both higher and more difficult to quantify. Future work should look into the measurement of other properties, such as speed of sound, to see if additional uncertainty reduction can be achieved.

REFERENCES

[1] Marion, John, et al. The STEP 10 MWe sCO_2 Pilot Plant Demonstration. Proceedings of ASME Turbo Expo 2019: Turbomachinery Technical Conference and Exposition, 2019.

[2] STEP Demo pilot plant achieves full operational conditions for Phase 1 of testing | Southwest Research Institute

[3] EXCEED GEO ENERGY & Peregrine Turbine Technologies Announce Collaboration to Deploy Breakthrough sCO_2 Geothermal Energy | Austin Daily Sun

[4] Echogen Announces Commercial Agreement to Deploy Grid-Scale Long Duration Energy Storage Technology

[5] Carbon TerraVault and Net Power Sign MOU to Develop Low Carbon, Reliable Power Solutions in California - Net Power

ACKNOWLEDGEMENTS

The authors would like to acknowledge and thank the hard work of the team members of SwRI, GE, GTI Energy, the Joint Industry Program members, and gratefully acknowledge the U.S. Department of Energy, Office of Fossil Energy and the National Energy Technology Laboratory, under Award Number DE-FE0028979.